EARTHQUAKE ENGINEERING AND STRUCTURAL DYNAMICS
Earthquake Engng Struct. Dyn. 2010; **39**:23–44
Published online 17 June 2009 in Wiley InterScience (www.interscience.wiley.com). DOI: 10.1002/eqe.931

Seismic rehabilitation performance of steel side plate moment connections

Chung-Che Chou[1,2,*,†,‡,§], Keh-Chyuan Tsai[1,2,¶,‖], Yuang-Yu Wang[3] and Chih-Kai Jao[4,**]

[1]*Department of Civil Engineering, National Taiwan University, Taipei, Taiwan*
[2]*National Center for Research on Earthquake Engineering, Taipei, Taiwan*
[3]*College of Civil Engineering, Tongji University, Shanghai, China*
[4]*Department of Civil Engineering, National Chiao Tung University, Hsinchu, Taiwan*

SUMMARY

Moment connections in an existing steel building located in Kaohsiung, Taiwan were rehabilitated to satisfy seismic requirements based on the 2005 AISC seismic provisions. Construction of the building was ceased in 1996 due to financial difficulties and was recommenced in 2007 with enhanced connection performance. Steel moment connections in the existing building were constructed by groove welding the beam flanges and bolting the beam web to the column. Four moment connections, two from the existing steel building, were cyclically tested. A non-rehabilitated moment connection with bolted web-welded flanges was tested as a benchmark. Three moment connections rehabilitated by welding full-depth side plates between the column face and beam flange inner side were tested to validate the rehabilitation performance. Test results revealed that (1) the non-rehabilitated existing moment connection made by *in situ* welding process prior to 1996 had similar deformation capacity as contemporary connection specimens made by laboratory welding process, (2) all rehabilitated moment connections exhibited excellent performance, exceeding a 4% drift without fractures of beam flange groove-welded joints, and (3) presence of the full-depth side plates effectively reduced beam flange tensile strain near the column face by almost half compared with the non-rehabilitated moment connection. The connection specimens were also modeled using the non-linear finite element computer program ABAQUS to further confirm the effectiveness of the side plate in transferring beam moments to the column and to investigate potential sources of connection failure. A design procedure was made based on experimental and analytical studies. Copyright © 2009 John Wiley & Sons, Ltd.

Received 20 June 2008; Revised 22 April 2009; Accepted 24 April 2009

KEY WORDS: rehabilitated steel moment connection; side plate; cyclic test; finite element analysis

*Correspondence to: Chung-Che Chou, Department of Civil Engineering, National Taiwan University, Taipei, Taiwan.
†E-mail: cechou@ntu.edu.tw
‡Associate Professor.
§Associate Research Fellow.
¶Professor of Civil Engineering.
‖Director.
**Former Graduate Student.

INTRODUCTION

A building utilizing traditional bolted web-welded flange moment connections can experience weld fracture during moderate or severe earthquakes, leading to insufficient ductility. Many traditional steel moment connections, which were fabricated following pre-Northridge construction practices with low notch toughness E70T-4 electrode, show minimal plastic deformation (e.g. 1% drift) before weld fracture at the beam-to-column interface [1–3]. The essence of all rehabilitated connections changes the relative strength ratio of a welding connection and the beam section near the column face to make beam yielding prior to fractures of a welding connection, consequently improving the ductility of an entire connection. Weakening schemes include the use of a reduced beam section or reduced flange plates near the beam-to-column interface to avoid groove weld fracture or beam buckling [4–6]. Strengthening schemes include the use of cover plates, upstanding ribs, and haunches near the beam-to-column interface [7–12]. The beam flanges near the column face can be rehabilitated to remain elastic, preventing groove weld fracture.

The ER70S-6 electrode, similar to the E71T-8 or E70TG-K2 electrodes, provides a minimum specified Charpy V-Notch value of 27 J at −29°C (20 ft-lbs at −20°F), which is accepted by AISC [13] for beam flange groove welds. Since the ER70S-6 electrode is used to conduct the beam flange groove welds to the box column in Taiwanese construction practices, the connection shows a better performance (e.g. 3% drift) than pre-Northridge moment connections utilizing the E70T-4 electrode. However, these connections still fail to satisfy connection performance requirements, specified based on AISC [13] and FEMA 350 [14]. When a composite slab is present in the existing building, introducing a reduced beam section, reduced flange plates, upstanding ribs, or cover plates near the beam-to-column interface cause slab damages. Although the welded haunch scheme eliminates the need to modify the existing top flange welds, reducing a clear height near the beam-to-column interface might cause discomfort to occupants. This study [15] thus provides a rehabilitation scheme for improving the cyclic performance of steel moment connections, minimizing interference from the composite slab, and reducing story height requirements in an existing steel building in Taiwan.

Construction of a 34-story steel hotel in Kaohsiung, Taiwan started in 1993 and the erection of the entire frame and the pouring of concrete slabs up to the 26th floor were completed before 1996. Owing to the financial difficulties faced by the developer, the construction of the original hotel was suspended for 10 years. Recently, this building has been rehabilitated for residential purposes. Since the original structural system could not meet new seismic requirements mandated in 2005, several retrofitting schemes were adopted in the reconstruction project to upgrade the seismic performance of the existing building. In some bays, buckling-restrained braces were added from the 1st to 11th floors, and eccentrically braced links were added from the 12th to 25th floors. All the existing moment connections, which were made based on the pre-Northridge-type details but with the high toughness electrode, were rehabilitated by adding a pair of full-depth side plates near the column face and inside the beam flanges without removing the concrete slab. A research [16] investigating the seismic demands for the existing and retrofitted buildings subjected to design-based and maximum-considered earthquakes confirmed the effectiveness of those retrofitting structural elements. The inelastic time-history analyses suggested that peak inter-story drifts of the original and the retrofitted structures reached about 1.2% and 1.4%, respectively, under maximum-considered earthquakes. The rotational demand imposed on the welded moment connection was about 1–1.5% for both the existing and retrofitted structures, smaller than the rotational capacity (2–3% drift) found in the tests of moment connection specimens prior to

DOI: 10.1002/eqe

1996 [17]. In their study [17], connection specimens used ASTM A36 steel beams with sections ranging from H530×160×10×14 (W21×50) to H545×315×13×20 (W21×101), smaller than those in the existing building. All flange groove welds were made in the laboratory with the specimen in an upright position to simulate field conditions. The weld electrode was E70T-7 made by Lincoln electric company and provided no specified level of toughness. Therefore, the performance of the existing moment connection was expected to exceed seismic demands according to inelastic time-history analyses of the building, but violate requirements based on the 2005 AISC seismic provisions [13]. The owner and the design engineer of the building made the performance set for rehabilitated moment connections to meet strength and ductility requirements (4% drift) prescribed in AISC seismic provisions [13].

Cyclic testing was performed on four exterior moment connections, two of which were removed from the existing steel building. A rehabilitation scheme was proposed to strengthen three connections by adding a pair of full-depth side plates between the column face and beam flange inner side. The side plates are intended to help transfer some beam moments to the column because the existing beam flange groove-welded joints could sustain modest inelastic deformation before fracturing [11, 17, 18]. No need is required to modify the existing groove welds of the beam top and bottom flanges, indicating no damages in an existing composite slab. This scheme differs from that utilizing the side plate connection [14], which completely eliminates the reliance on existing beam flange groove-welded joints at the column face for transferring beam moments.

In this paper, weld and fabrication details, which represent the existing connection specimens, are presented first. Test results show that the actual performance of the existing moment connections before and after rehabilitation is then presented to validate the rehabilitation scheme. The effects of *in situ* welding and laboratory welding processes on connection performance are also studied. Finally, the connection specimens are modeled using the non-linear finite element computer program ABAQUS [19] to confirm the effectiveness of the side plate in transferring beam moments to the column and to investigate potential sources of connection failure. A step-by-step design procedure is presented based on the test and analytical results.

REHABILITATED MOMENT CONNECTION

Figure 1 shows a rehabilitated moment connection using a pair of side plates between the column face and the beam flange inner side. These two plates are used to transfer some beam flange force to the column to reduce beam flange strain and prevent groove weld fracture. The figure shows moment demand, M_{dem}, along the beam, assuming that a plastic hinge is located at a quarter beam depth from the end of the side plates. This location is used based on the FEMA 350 [14] recommendation for connections reinforced with either cover plates or welded haunches. The moment at the column face, as determined by projecting moment capacity M_{PH} at the plastic hinge location, is

$$M_{\text{dem}} = \frac{L_{\text{b}}}{L_{\text{b}} - (L_{\text{s}} + d_{\text{b}}/4)} M_{\text{PH}} = \frac{L_{\text{b}}}{L_{\text{b}} - (L_{\text{s}} + d_{\text{b}}/4)} (\beta R_{\text{y}} \sigma_{\text{yn}} Z_{\text{b}}) \tag{1}$$

where L_{b} is the distance from the mid-span to the column face, L_{s} is the side plate length, d_{b} is the beam depth, Z_{b} is the plastic section modulus of the beam, σ_{yn} is the specified yield strength of the steel, R_{y} is the material over-strength coefficient, and coefficient β denotes strain hardening [14]. Since steel properties were obtained from tensile coupon tests before fabricating rehabilitated

DOI: 10.1002/eqe

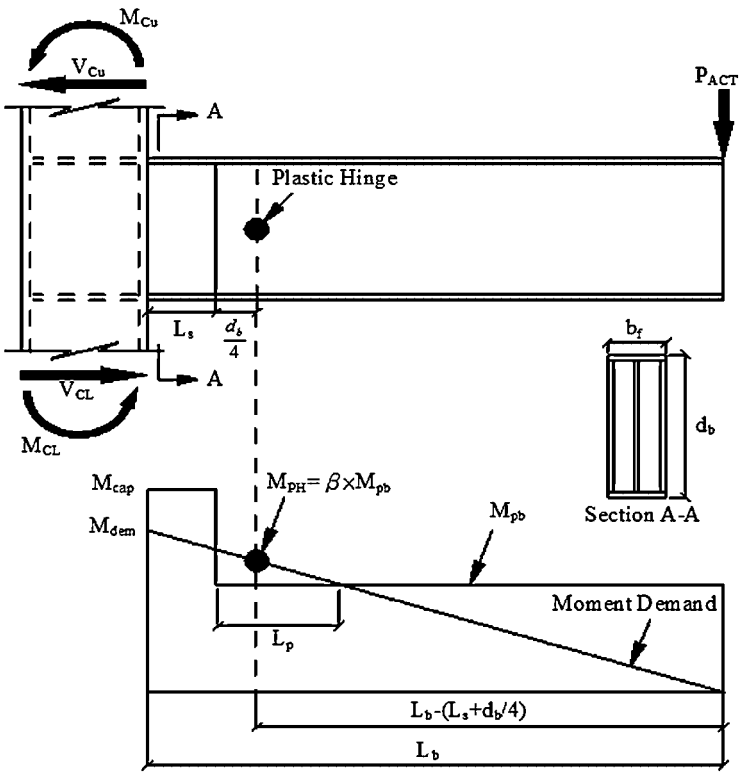

Figure 1. Moment capacity and demand along a beam axis.

specimens, actual yield strength, tensile strength, and $R_y = 1$ were used in Equation (1) to estimate the moment demand, M_{dem}.

Moment capacity, M_{cap}, near the beam-to-column interface increases as a result of the side plates. Although the stress distributions near the beam-to-column interface are complicated, a simple bending theory is adopted to estimate the flexural capacity of the rehabilitated beam, which is the summation of the flexural strengths of the beam, M_{pb}, and the two side plates, M_{ps}

$$M_{cap} = M_{pb} + M_{ps} = Z_b R_y \sigma_{yn} + \tfrac{1}{2}(d_b - 2t_f)^2 R_y \sigma_{yn} t_s \tag{2}$$

where t_f is the beam flange thickness and t_s is the side plate thickness. It is assumed that the side plates are subjected to the top and bottom flange force, P_{sF}, as shown in Figure 2(b), and exhibit a fully plastic stress state (Figure 2(c)). By considering moment equilibrium in the side plate, the force, P_{sF}, is:

$$P_{sF} = \frac{F_s[\frac{1}{2}(d_b - 2t_f)]}{d_b - 2t_f} = \tfrac{1}{4}(d_b - 2t_f) R_y \sigma_{yn} t_s \tag{3}$$

DOI: 10.1002/eqe

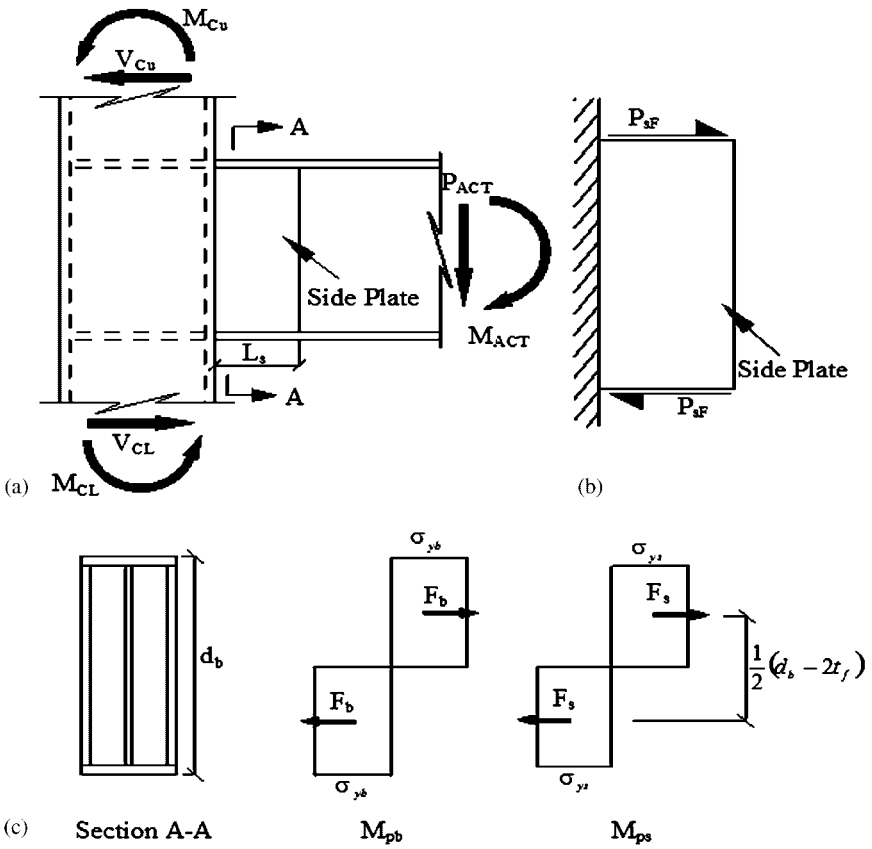

Figure 2. Side plate flexural stress state: (a) elevation; (b) side plate; and (c) stress distribution.

Additionally, the force P_{sF} is transferred to the side plate through shear on the groove-welded joint between the side plate and beam flange inner side, and thus the minimum length of the side plate, L_s, is determined based on groove weld strength

$$L_s \geqslant \frac{\frac{1}{4}(d_b - 2t_f) R_y \sigma_{yn}}{0.8(0.6F_{exx})} \tag{4}$$

where F_{exx} is the weld strength. Assuming that the rehabilitated beam moment capacity–demand ratio, $\alpha(=M_{cap}/M_{dem})$, is larger than one, the side plate thickness, t_s, can be calculated using Equation (2):

$$t_s \geqslant \frac{\alpha M_{dem} - M_{pb}}{\frac{1}{2}(d_b - 2t_f)^2 R_y \sigma_{yn}} \tag{5}$$

DOI: 10.1002/eqe

When these two side plates are added to the beam-to-column interface, the strong column–weak beam criterion should also be checked

$$\gamma = \frac{\sum Z_c(\sigma_{yn} - \sigma_a)}{\sum M_c} > 1 \tag{6}$$

where Z_c is the plastic section modulus of the column above and below the connection, σ_a is the axial stress in the column above and below, and M_c is the sum of the column moments resulting from the development of the probable beam plastic moment M_{PH} within each beam that frames into the connection. It can be computed using

$$\sum M_c = n\left[M_{PH}\frac{L_b + d_c/2}{L_b - (L_s + d_b/4)} + V_g\left(\frac{d_c}{2} + L_s + \frac{d_b}{4}\right)\right]\frac{H_c - d_b}{H_c} \tag{7}$$

where H_c is the column length measured from top and bottom inflection points, d_c is the column depth, V_g is the beam shear at the plastic hinge location produced by gravity load in beam span, and n is equal to 1 and 2 for the exterior and interior moment connections, respectively.

TEST PROGRAM

Connection specimens

The experimental program consisted of tests of four specimens, each of which represented an exterior moment connection with one steel beam and one welded box column. Table I lists the beam, column, and side plate sizes. The column width is 2.2–2.8 times the beam width, and the column thickness is 1.25–1.67 times the beam flange thickness. The column has continuity plates as thick as the beam flange. ASTM Grade 50 steel was utilized for the column, continuity plate, and side plate; ASTM A36 steel was utilized for the beam. The specimens UR and SP1 were removed from the 33rd floor of an existing steel building located in Kaohsiung, Taiwan, whereas Specimens SP2 and SP3 were fabricated in the laboratory. Specimen UR represented an unreinforced bolted web-welded flange fully restrained moment connection (Figure 3(a)) and was tested as a benchmark.

Specimen SP2 (Figure 3(b)) was identical to Specimen SP3, except that (1) the side plate size was 22×300 mm in the Specimen SP2 and 18×254 mm in the Specimen SP3, and (2) Specimen SP3 had side plate length, L_s, less than the required value of 264 mm based on Equation (4). The objective was to discover the possible failure mode in the rehabilitated connection. Table II lists information for beam moment capacity, demand, and values of α, β, and γ. The rehabilitated beam moment capacity–demand ratio, $\alpha(=M_{cap}/M_{dem})$, is varied to study the effects of reinforcement on connection cyclic behavior and to discover the minimum reinforcement for the proposed connection. The strong column–weak beam ratio, γ, according to Equation (6) is high because only one beam plastic moment and no axial stresses in the column are considered to represent the test specimen condition.

Welding and fabrication details for existing and laboratory moment connections

All the real and lab specimens were welded by the self-shielded flux-cored arc welding process using the ER70S-6 electrode. This electrode, which is similar to the E71T-8 or E70TG-K2 electrodes,

DOI: 10.1002/eqe

Table I. Member sizes and properties.

Spe	Column size/beam size	Column strength		Beam flange strength		Beam web strength		Side plate size	Side plate strength	
		σ_y^* (MPa)	$\sigma_u^\dagger$ (MPa)	σ_y (MPa)	σ_u (MPa)	σ_y (MPa)	σ_u (MPa)	($t_s \times L_s$)	σ_y (MPa)	σ_u (MPa)
UR	$700\times700\times35\times35$ $H702\times254\times16\times28$	391	525	275	485	288	495	—	—	—
SP1	$700\times700\times35\times35$ $H688\times255\times13\times21$	391	525	250	418	385	437	20×300	400	557
SP2	$550\times550\times35\times35$ $H702\times254\times16\times28$	385	530	250	418	280	437	22×300	370	500
SP3	$550\times550\times35\times35$ $H702\times254\times16\times28$	385	530	251	413	281	434	18×254	400	532

*Actual yield strength.
†Actual tensile strength.

DOI: 10.1002/eqe

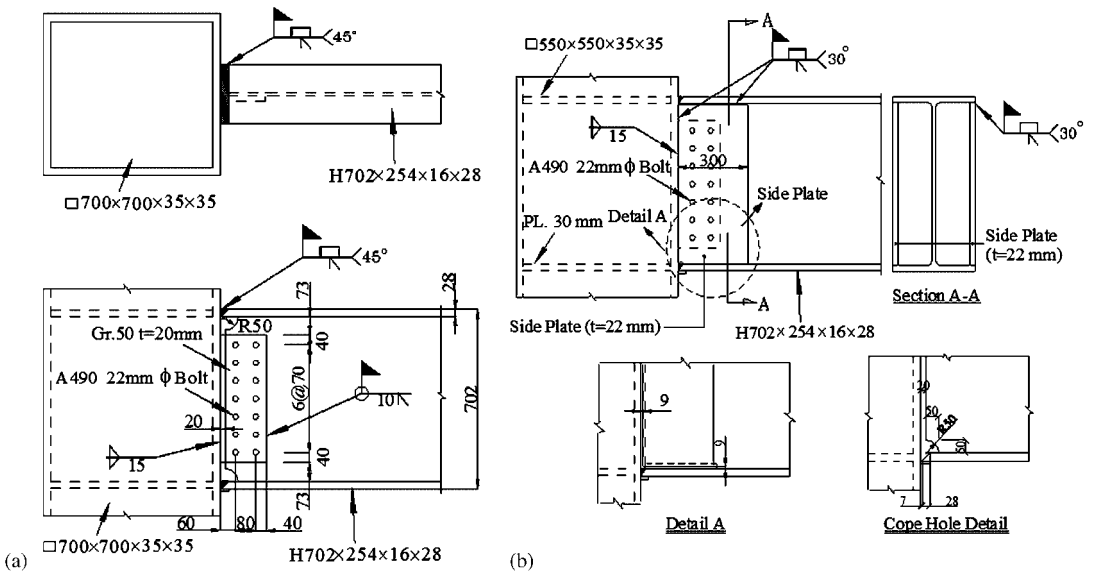

Figure 3. Connection details: (a) Specimen UR and (b) Specimen SP2.

Table II. Beam moment capacity–demand ratio after rehabilitation.

Specimen	β	M_{pb} (kN m)	M_{PH} (kN m)	M_{dem} (kN m)	M_{ps} (kN m)	M_{cap} (kN m)	α	γ
SP1	1.34	1273	1705	1969	1669	2942	1.49	7.5
SP2	1.34	1666	2232	2572	1699	3364	1.31	3.5
SP3	1.32	1672	2207	2506	1502	3175	1.27	3.6

provides a minimum specified Charpy V-Notch value of 27 J at −29°C (20 ft-lbs at −20°F). Real Specimens UR and SP1, removed from the 33rd floor of the existing building, were constructed based on the typical construction practice in Taiwan prior to 1996. First, the steel beam was positioned to the column shear tab and the web bolts were installed and fully tensioned. The backing bar projected 50 mm beyond the both sides of the beam flange and weld tabs was attached next to the beam flange. The beam flanges were then groove welded to the column flange. Each pass of flange groove welds was initiated, and terminated when possible, at a point outside the flange. This was done to prevent poor-quality welds, which normally occur at the initiation of the weld at the beam flange-to-column face. Finally, supplemental welds between the shear tab and the beam web were conducted. For Specimen SP1, complete-penetration single-bevel groove welds were used to connect the side plate to the beam and column flanges. Each pass of side plate to beam flange groove welds was initiated at a point outside the side plate and terminated at a point at the column flange. Each pass of side plate to the column flange groove welds was then initiated from the beam bottom flange and terminated at the beam top flange. All backing bars used for the groove welds were left in place after welding was complete. Ultrasonic tests (UT) were conducted for all flange groove welds, and they all satisfied the prescribed acceptance criteria [20].

DOI: 10.1002/eqe

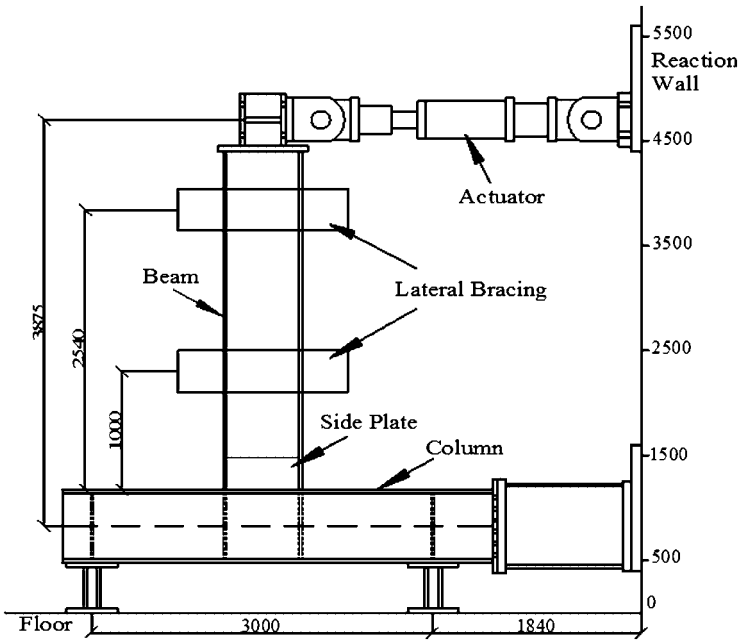

Figure 4. Test setup.

Lab welds for Specimens SP2 and SP3 were made by a fabrication shop welder, using weld positions typical to shop welding. More specifically, beam flange to column groove welds were made with the specimen oriented to permit flat position welding. Because the column was placed horizontally, each pass of side plate to column flange groove welds was conducted before each pass of side plate to beam flange groove welds. Each pass of side plate to beam flange groove welds was initiated at a point at the column face and terminated at a point outside the side plate. Supplemental fillet welds between the shear plate and the beam web were not adopted, and weld tabs were also not used for the beam flange groove welds. The backing bars, which were about 60 mm wider than the beam flange width, remained in place after the welding was complete. For all specimens, a fillet weld, helping to reduce the notch effect of a left in place backing bar from a theoretical perspective, was not made between the backing bar and the column.

Test setup and loading protocol

The exterior connection specimens were tested as shown in Figure 4. Restraint to lateral-torsional buckling of the beam was provided near the actuator and at a distance of 1000 mm from the column face. Displacements were imposed on the beam by a 1000 kN actuator at a distance of 3875 mm from the column centerline. The AISC cyclic displacement history [13] was used and run under displacement control. The inter-story drift, which was computed by the actuator displacement divided by the distance to the column centerline, was used as the control variable. Specimens were tested until connection failure occurred or limitations of the test setup were reached.

DOI: 10.1002/eqe

TEST RESULTS

Non-rehabilitated existing moment connection

Figure 5(a) shows the global response of Specimen UR; the moment computed at the column face is normalized by the nominal plastic moment of the beam, M_{np}. Minor whitewash flaking, indicating beam yield, was observed in the beam flange near the groove weld at an inter-story drift of 0.75%. At an inter-story drift of 1.5%, significant yielding was observed along the weld boundary of the beam top portion, which included points at the edge of the beam flange adjacent to the groove weld, the edge of the shear plate adjacent to the fillet weld on the column flange, and the toe of the weld access hole. Minor fractures were initiated at these three points at an inter-story drift of 3%, but no fracture was observed in the beam bottom portion. Deterioration in the overall strength of the specimen was not observed until the fractures propagated across almost the full flange width (Figure 6(a)) and 140 mm long along the shear plate edge (Figure 6(b)) at a −4% drift. Note that these fractures initiating adjacent to the edge of the *in situ* weld extended in a stable manner in the base metal (heat-affected zone). A crack initiating at the toe of the weld access hole did not propagate. This beam flange failure mode was similar to that observed in prior tests of connection specimens [17]; all the flange welds in these specimens were made in the laboratory by a certified shop welder in simulating *in situ* welding conditions. After top flange fracture, the specimen was reversely loaded to an inter-story drift of 4% so that the beam bottom flange was in tension. A minor crack was initiated at the toe of the weld access hole, but no crack was initiated at the heat-affected zone of the beam bottom flange or the shear plate. No visible sign of yielding in the column panel was observed during the test. Based on observed performance in Specimen UR, it is judged that this specimen made by *in situ* welding process prior to 1996 and accepted by the UT examination has similar deformation capacity as contemporary connection specimens made by the lab welding process [17]. It suggests that the use of high toughness electrodes is highly beneficial. Even if a reduction of toughness is suffered due to improper welding conditions (field versus laboratory), a substantially high level of toughness can still remain, leading to moderate deformation capacity of the beam. Although the existing connection specimen before rehabilitation shows good performance, exceeding seismic demands (1–1.5% drift) obtained from inelastic time history analyses of the steel frame [16], it fails to satisfy a current ductility requirement (4% drift) prescribed in AISC seismic provisions [13]. It also indicates that the drift requirement per AISC seismic provisions [13] is seemingly too stringent and may be investigated for a proper limit.

Rehabilitated moment connection

Figure 5(b) shows the hysteretic responses of Specimen SP1, which achieved high inter-story drift without welded joint fracture. Specimen SP1 was removed from the existing steel building and retrofitted with two side plates in the field. Unlike Specimen UR, the beam flange near the groove weld showed no sign of yielding during initial loading. Instead, the beam flange near the end of the side plate yielded at an interstory drift of 0.75–1%. Beam flange yielding expanded with increasing drift and the beam flange adjacent to the column groove weld showed sign of yielding at an inter-story drift of 2%. Crack initiation as observed in Specimen UR test was not detected in Specimen SP1 test at an inter-story drift of 3%, where beam flange and web local buckling outside the side plate commenced. Local buckling was accompanied by a twisting of the beam outside the side plate, and resulted in a gradual reduction in the specimen capacity at an inter-story drift of 4%. Finally, the flange local buckling initiated tearing of the beam flange immediately adjacent

DOI: 10.1002/eqe

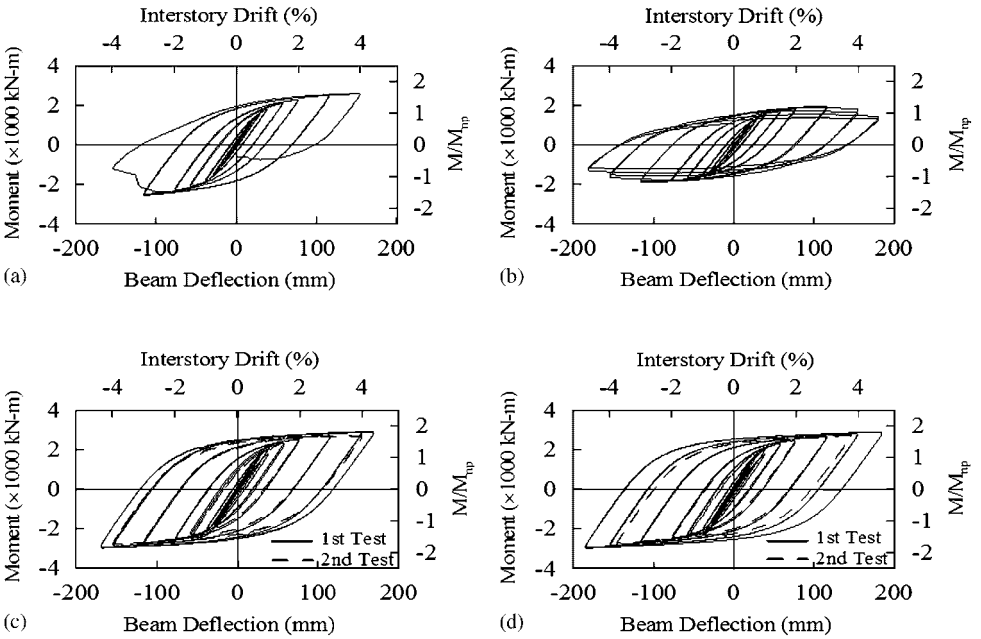

Figure 5. Beam moment-deflection responses: (a) UR; (b) SP1; (c) SP2; and (d) SP3.

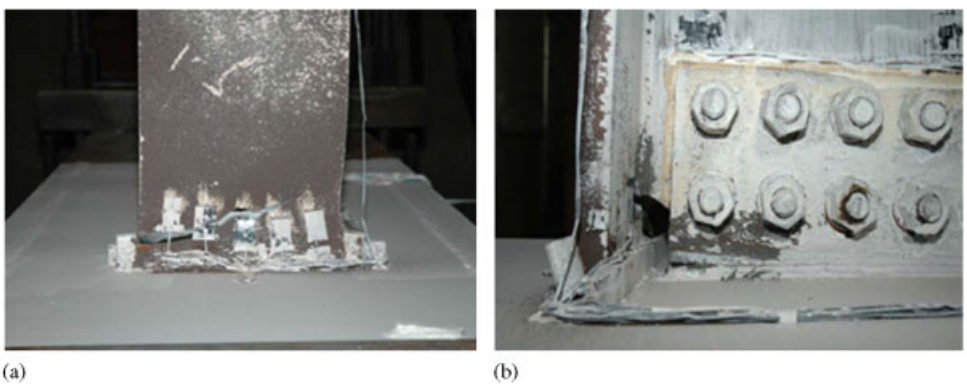

Figure 6. Specimen UR failure modes (−4% drift): (a) beam top flange fracture and (b) shear plate fracture.

to the edge of the side plate groove weld. After the beam finished two cycles of a 4.7% drift, testing was stopped due to limitations in the test setup. Fractures as observed in non-rehabilitated Specimen UR were not found in this specimen at the end of testing (Figure 7), indicating that two side plates near the column face can improve seismic performance of the actual connection made by *in situ* welding process prior to 1996.

DOI: 10.1002/eqe

Figure 7. Specimen SP1 beam buckling (4.7% drift).

Beam flange to column groove welds in Specimens SP1 and SP2 were made in the existing building prior to 1996 and laboratory in 2007, respectively. Moreover, the rehabilitated beam moment capacity–demand ratio, α, was lower in Specimen SP2 than Specimen SP1. The beam flange of Specimen SP2 near the groove weld and the end of the side plate yielded at an inter-story drift of 0.75–1%. The side plate near the junction of the beam flange and column showed yielding at an inter-story drift of 3%. Figure 8(a) shows the beam deformation of Specimen SP2 during the first test to an inter-story drift of 4.4%; flange and web buckling amplitudes were about 14 mm and 16 mm, respectively, much smaller than those observed in Specimen SP1 test. A crack, as noted in Specimen UR, was also observed at edges of the beam top and bottom flanges adjacent to the groove welds (Figure 8(b)), but deterioration in the overall strength of the specimen was not observed at the end of test. This crack was not observed in Specimen SP1 with large reinforcement, suggesting that the moment capacity–demand ratio (or side plate size) may have played an important role in reducing stress concentration. It is unclear how severe this stress concentration is and under what circumstances it may become a significant factor in rehabilitated connection performance. Therefore, Specimen SP2 was retested instead of loading to a larger drift due to limitations in the test setup. When Specimen SP2 was retested to an inter-story drift of 1%, flange cracks near the end of the side plates, as noted in Specimen SP1 test at a 4.7% drift, were observed. This crack length increased to 10 mm (Figure 9(a)) after finishing two cycles of a 4% drift; significant beam buckling was also noted (Figure 9(b)), leading to slight strength degradation (Figure 5(c)). The cracks as noted at edges of the beam flanges adjacent to the groove welds during the first test (Figure 8(b)) did not expand and affect the connection cyclic performance during the second test. No weld fracture and no column panel zone yielding were observed after the second test. Having observed cyclic performance in rehabilitated Specimens SP1 and SP2 further confirms that as long as the high toughness electrode is used with side plate reinforcement, specimens made either in the field or laboratory exceed a drift requirement of 4% per AISC seismic provisions [13]. Note that Specimen UR made by using the high toughness electrode alone cannot ensure the satisfaction of the concerned drift requirement of 4%.

Specimen SP3 was identical to Specimen SP2 except that Specimen SP3 had a small side plate and an insufficient side plate length (Table I). No beam buckling was observed after the specimen finished 4% drift cycles. However, a minor crack was observed at the edge of the groove weld between the beam flange inner side and the side plate. Beam buckling was difficult to detect even

DOI: 10.1002/eqe

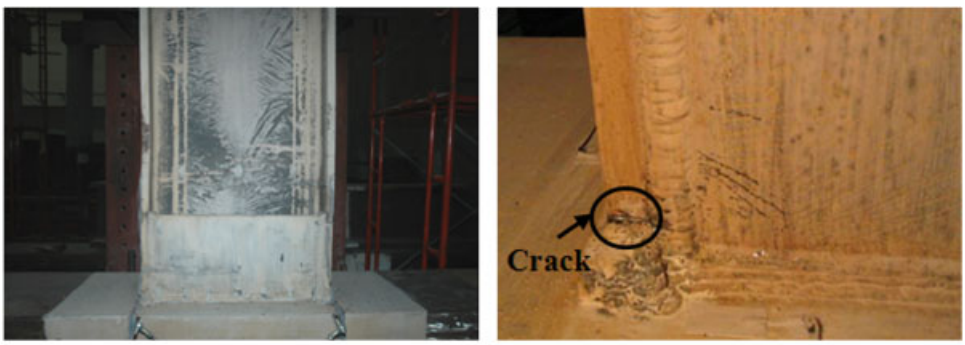

Figure 8. Specimen SP2 beam and side plate yielding during the first test to a 4.4% drift: (a) beam yielding and buckling and (b) side plate yielding and beam flange crack.

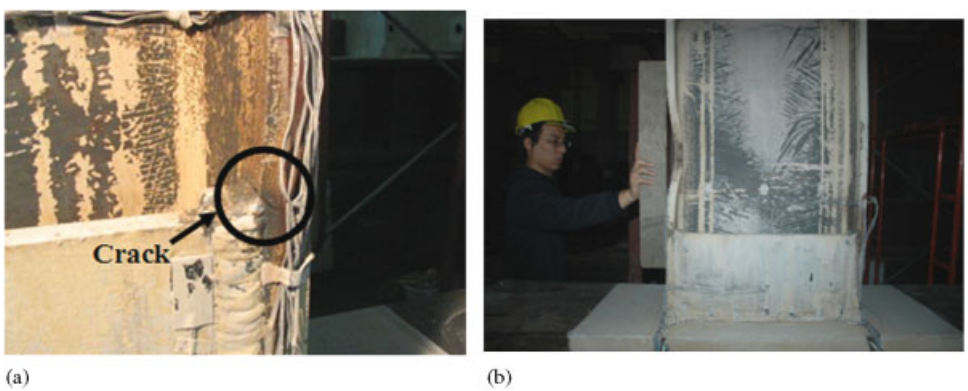

Figure 9. Specimen SP2 after the second test (4% drift): (a) flange crack at end of side plate and (b) beam buckling.

when testing to an inter-story drift of 4.8%. Comparison of all rehabilitated specimens showed larger flange and web buckling with larger reinforcement. When Specimen SP3 was retested at an inter-story drift of 1%, a crack, not found in other specimen tests, was observed near the beam-to-column groove-welded joint. This crack did not expand after finishing 3.77% drift cycles. However, the crack, initiated at the edge of the side plate to beam flange inner side groove weld, ran horizontally along the weld due to the beam flange local buckling. The crack length was 70 mm at the end of the second test (Figure 10), and slight strength degradation was also noted in the hysteretic loops (Figure 5(d)). This fracture was not observed in Specimen SP1 and SP2 tests due to sufficient weld length (Table I).

Table III lists moment demands, M_{dem} and M_{PH}, calculated by multiplying the actuator force and the distance to the column face and plastic hinge location, respectively. The flexural strengths, M_{cap} and M_{pb}, were calculated using true material strength according to Equation (2). The rehabilitated beam moment capacity–demand ratio, $\alpha(=M_{\text{cap}}/M_{\text{dem}})$, ranges from 1.11 to 1.56, whereas the strain-hardening coefficient β ranges from 1.28 to 1.54. Note that the Specimen SP1 has smallest β

DOI: 10.1002/eqe

Figure 10. Specimen SP3 test observation (after second test).

Table III. Parameters α and β based on test results.

		Moment demand (kN m)		Flexural strength (kN m)		Parameters α and β	
Specimen	Interstory drift (%)	Column face M_{dem}	Plastic hinge M_{PH}	Column face M_{cap}	Plastic hinge M_{pb}	$\alpha=\frac{M_{cap}}{M_{dem}}$	$\beta=\frac{M_{PH}}{M_{pb}}$
UR	+3	2516	2516	1799	1799	0.72	1.4
	−3	−2517	−2517			0.72	1.4
SP1	+4	1885	1633	2942	1273	1.56	1.28
	−4	−1952	−1691			1.51	1.33
SP2	+4	2948	2559	3364	1666	1.14	1.54
	−4	−2896	−2514			1.16	1.51
SP3	+4	2866	2524	3175	1672	1.11	1.51
	−4	−2830	−2492			1.12	1.49

value among all of the specimens because of significant beam buckling, limiting strain hardening. However, minor beam buckling was observed in Specimens SP2 and SP3 in the first test, leading to β values of approximately 1.5, higher than that calculated based on FEMA 350 (Table II). Note that for high column flexural stiffness and high reinforcement near the beam-to-column interface ($\alpha>1.5$ for Specimen SP1 in Table III), the beam buckling amplitude is large and the rate of degradation of moment resistance is high in the first test. Conversely, when a column is relatively soft with a relatively low reinforcement near the beam-to-column interface ($\alpha=1.11-1.16$ for Specimens SP2 and SP3 in Table III), the beam buckling amplitude is much smaller and the rate of degradation of moment resistance is also slower in the first test.

Beam flange strain

The effectiveness of the side plate in decreasing beam flange tensile strain can be observed from the measured strains at 60 mm from the column face (Figure 11). At an inter-story drift of 3%, the tensile strains in the beam top and bottom flanges of the non-rehabilitated Specimen

DOI: 10.1002/eqe

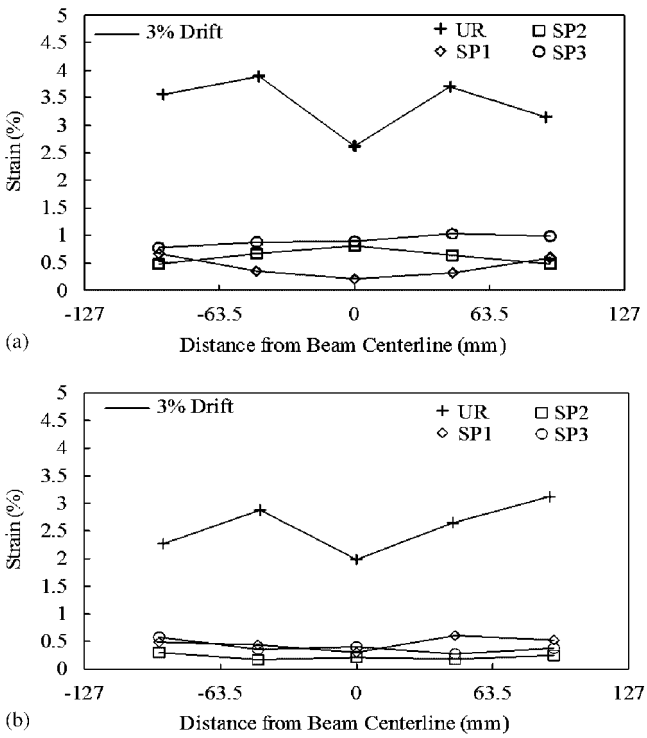

Figure 11. Beam flange tensile strains (3% drift): (a) top flange and (b) bottom flange.

UR significantly exceeded those of the rehabilitated specimens. The tensile strains in Specimen SP2 were lower than those in Specimen SP3, indicating that increasing plate thickness effectively reduced tensile strains. Furthermore, modest beam yielding near the column face has no adverse effects on the connection seismic performance. The maximum flange strain at the assumed plastic hinge location, 430 mm from the column face in Specimen SP3, was 2.2% ($=16\varepsilon_y$) at an inter-story drift of 4%, demonstrating successful relocation of the plastic hinge to a quarter beam depth from the end of the side plate.

Side plate strain

Figure 12 shows the measured longitudinal strains along the side plate depth, located 35 mm from the column face. The longitudinal strains in the side plate center portion are small, indicating ineffective in transferring beam flange forces to the column. However, the longitudinal strains in the side plate near the beam flanges are greater than the yield strain, indicating effective in transferring beam flange forces. Because Specimen SP3 has thinner side plates than Specimen SP2 (Table I), the tensile strains in the side plate are higher in Specimen SP3 than in Specimen SP2. The maximum measured tensile strains at an inter-story drift of 4% were 0.5% ($2.7\varepsilon_y$) and 0.67% ($3.4\varepsilon_y$) for Specimens SP2 and SP3, respectively. A work [21] utilizing only a small part of side plates near the beam flange inner side to retrofit moment connections also confirmed the effectiveness of the rehabilitation scheme.

DOI: 10.1002/eqe

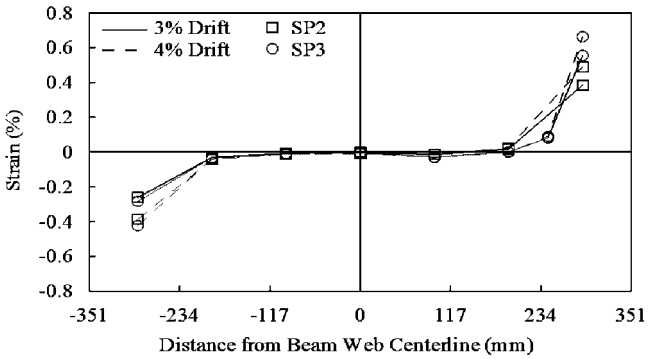

Figure 12. Side plate longitudinal strain profiles (35 mm from the column face).

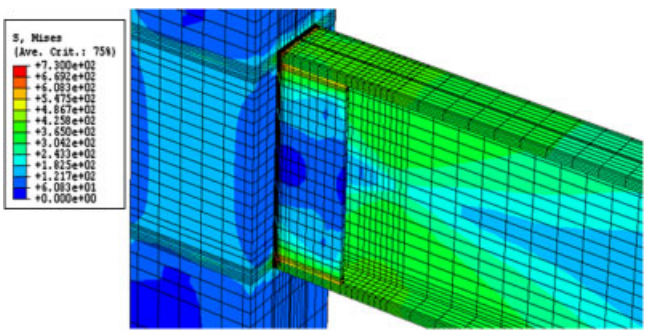

Figure 13. Specimen SP2 von Mises stress (3% drift).

FINITE ELEMENT STUDY

Finite element analysis was undertaken to study the cyclic behavior of rehabilitated moment connections. The objective was to verify test results, discover flexural contribution of the side plates, and study sources of potential failure mode. The specimen was modeled using eight-node brick elements C3D8R with reduced integration [19]. Coordinates common to components joined by the shear tab and beam web were constrained so as to have identical displacements. The groove welds joining the beam flange and column, and joining the side plates to the column and beam flanges were modeled, but the steel backing and weld access hole were not modeled. Only the geometry and material property of groove welds were considered in the model. Based on the material test report provided by the China Electric Company, Taiwan, the ER70S-6 electrode had yield and tensile strengths of 469 and 563 MPa, respectively, and elongation of 29%. The analyses accounted for material non-linearities, using the von Mises yield criterion. Figure 13 shows von Mises stress contours of Specimen SP2 at an interstory drift of 3%, indicating stress concentration near the top and bottom sides of the side plate.

Figure 14 compares beam moment-deflection hysteretic responses from testing and analysis. Initial stiffness, post-yield stiffness, and moments at the column face show good agreement. The

DOI: 10.1002/eqe

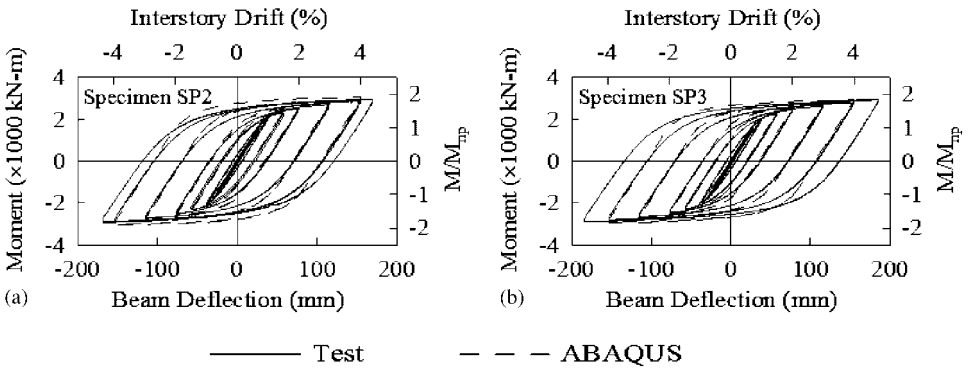

Figure 14. Hysteretic response comparisons between test and finite element model.

predicted longitudinal strains along the side plate depth, located 35 mm from the column face, correlate well with the test data (Figure 15). From the finite element model, moment, M_S, transferred through the side plate to the column, was computed based on the longitudinal stresses in the side plate, the respective area along the depth, and the distance to the beam web centerline. The ratio of M_S to the plastic moment strength of the side plate, M_{ps}, increased with drift (Figure 16(a)), and the ratios at an inter-story drift of 4% were 69 and 72% for Specimens SP2 and SP3, respectively. The ratio of M_S to the beam moment, M_{ABA}, computed at the column face, was 36–38% at an interstory drift of 4% (Figure 16(b)), indicating that about one third of the beam moment was transferred to the column through the side plates, and Specimen SP2 utilizing thicker side plates than Specimen SP3 transferred larger beam moments.

The rupture index (RI) was computed at different locations of the connection from ABAQUS results to assess the possible fracture source. Locations in a connection with higher values for RI have a greater potential for fracture [22]. Figure 17(a) shows three possible fracture locations observed in the tests: the beam flange top surface located 60 mm from the column face (Line A), the groove-weld top surface near the column face (Line B), and the beam flange inner side along the side plate weld (Line C). The side plate can significantly reduce the RI values at the beam flange (Figure 17(b)). However, the maximum RI for Specimens SP2 and SP3 at both ends of the beam flange groove weld is higher than for Specimen UR (Figure 17(c)), corresponding to a minor crack shown in Figure 8(b). Although the high RI value existed at both weld edges of the beam flange, the cracks, as noted in Specimens SP2 and SP3, did not propagate during tests and did not adversely affect the connection cyclic performance. The RI at the end of the side plate is also large (Figure 17(d)), indicating the possible source of the fracture observed in Figure 9(a).

SUMMARY OF SIDE PLATE MOMENT CONNECTION DESIGN PROCEDURE

A design procedure for the seismic rehabilitation of a bolted web-welded flange moment connection is developed based on experimental and analytical studies in this research [15]. The details of a non-rehabilitated fully restrained moment connection are: (1) beam flange groove welds are made using a high notch toughness electrode (e.g. ER70S-6, E71T-8, or E70TG-K2 electrodes) with steel backing left in place, (2) the beam web is bolted to the column shear plate without supplemental

DOI: 10.1002/eqe

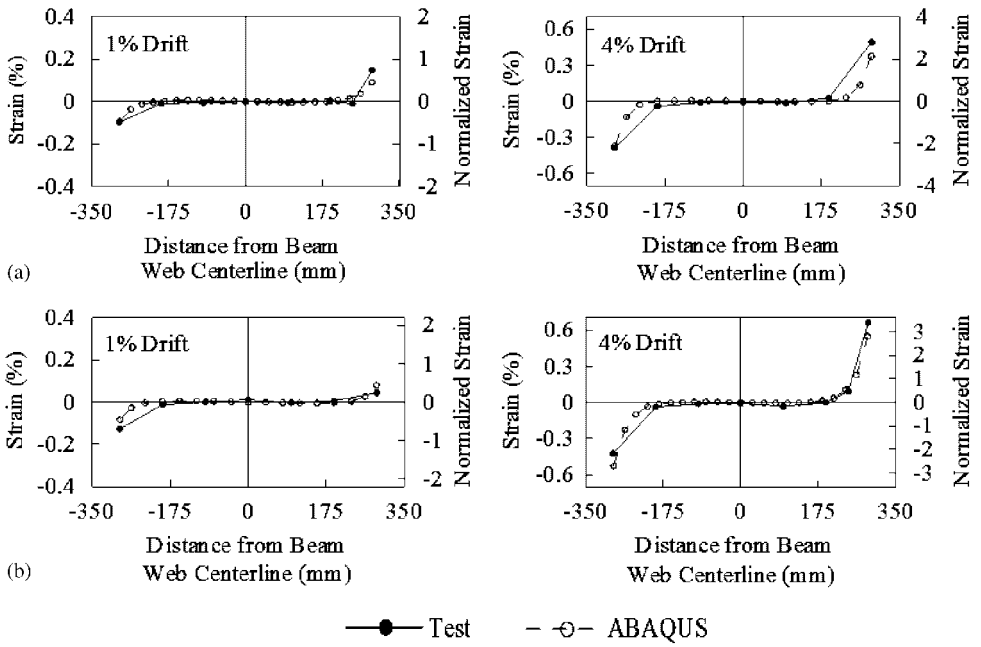

Figure 15. Side plate strain comparisons between test and finite element model: (a) Specimen SP2 and (b) Specimen SP3.

fillet welds between the shear plate and the beam web, and (3) continuity plates in the box column are as thick as the beam flange. Owing to the limited test data available for this type connection, the box column width should be less than 2.8 times the beam width, and the column thickness should be larger than 1.25 times the beam flange thickness to maintain locally stiff column relative to the beam. The step-by-step design procedure is summarized as follows:

Step 1: Select a side plate length, L_s, based on the beam dimension and strength (Equation (4)).

Step 2: Compute the beam plastic moment at the column face using a strain hardening factor, β, of 1.5 (Equation (1)).

Step 3: Use Equation (5) to compute the side plate thickness with a rehabilitated beam moment capacity–demand ratio, α, of 1.11–1.16.

Step 4: Check for strong column–weak beam condition (Equation (6)).

CONCLUSIONS

Four exterior moment connection specimens, each composed of an ASTM A572 Gr. 50 welded box column and an ASTM A36 wide-flange beam, were cyclically tested. Two bolted web-welded flange moment connections were removed from the existing steel building in Taiwan. One of the connections was rehabilitated by welding two side plates between the column face and the inside of the beam flange to improve seismic performance. Additional two rehabilitated moment connection specimens were fabricated in the laboratory. Note that the ER70S-6 electrode, which

DOI: 10.1002/eqe

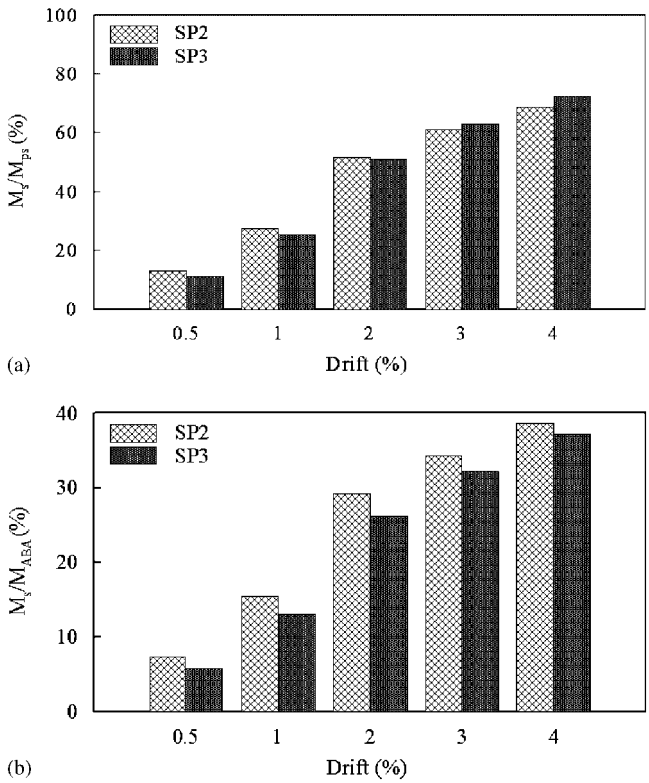

Figure 16. Side plate moment contribution: (a) plastic moment ratio and (b) moment contribution ratio.

is similar to the E71T-8 or E70TG-K2 electrodes, was used to make beam flange groove welds in all connections based on construction practices in Taiwan. Steel backing was left in place for the top and bottom flanges and no supplemental fillet welds were made between the steel backing and the column face. The following can be concluded based on the experimental and finite element analysis results:

1. Fracture of the beam flange near the column face was the failure mode for the non-rehabilitated Specimen UR. The inter-story drift angle was 3% and the maximum tensile strain was about 3–4%.
2. Based on the cyclic performance in Specimen UR, it is judged that this existing connection specimen made by *in situ* welding process before 1996 and qualified by the UT test has similar deformation capacity as contemporary connection specimens [17] made by the lab welding process. This can also be confirmed from tests of Specimens SP1 and SP2, which were made in the field and laboratory, respectively. These two specimens showed excellent cyclic performance, achieving a high inter-story drift without fracture of the beam groove-welded joint. It suggests that the use of high toughness electrodes is highly beneficial. Even if a reduction of toughness is suffered due to improper welding conditions (field versus laboratory), a substantially high level of toughness can still remain. However, such connection

DOI: 10.1002/eqe

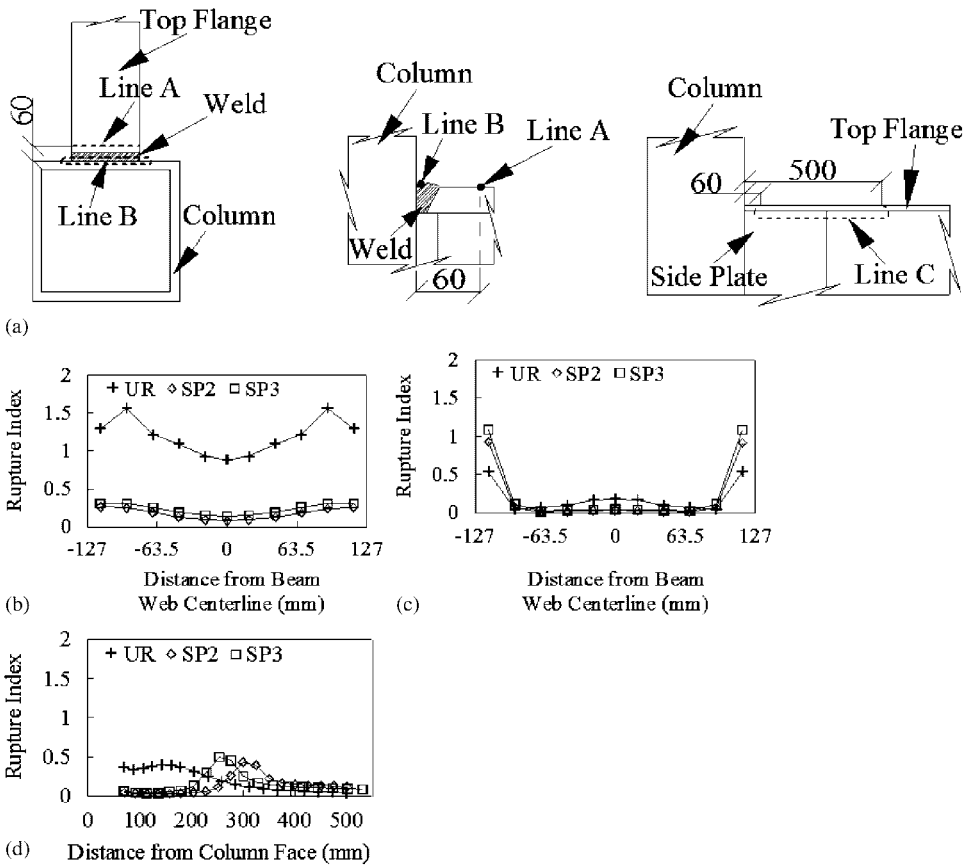

Figure 17. Comparison of rupture index at a 3% drift: (a) location; (b) Line A; (c) Line B; and (d) Line C.

without rehabilitation still fails to meet stringent requirements (4% drift) prescribed in AISC seismic provisions [13].

3. Maximum moment developed at a quarter beam depth from the end of the side plate was 1.28–1.54 times the actual beam plastic moment. The strain hardening of around 1.5 exceeded that calculated based on FEMA 350 [14] due to minor beam buckling at the plastic hinge location. In the absence of additional connection tests, a strain hardening factor of 1.5 for A36 beams was recommended for estimating the rehabilitated connection moment at the plastic hinge location.
4. The flexural capacity of the rehabilitated beam was the sum of the plastic moments of a non-rehabilitated beam and two side plates. The rehabilitated beam moment capacity–demand ratio, α, at the column face ranged from 1.11–1.56 for three rehabilitated connection specimens at an inter-story drift of 4%. For Specimen SP1, which had an α value larger than 1.5, significant beam buckling was observed in the first cyclic test at an inter-sotry drift of 4.8%, but no weld fracture was observed at the beam-to-column interface. For Specimens SP2

DOI: 10.1002/eqe

and SP3, which had α values ranging from 1.11–1.16, minor beam buckling was observed in the first cyclic test after an inter-story drift exceeded 4%. These specimens were retested using the same AISC cyclic loading protocol, and no fracture of the beam flange groove-welded joint at the column face was observed after the second test. However, because Specimen SP3 had insufficient side plate length, the weld fractured along the junction between the side plate and beam flange inner side. It is recommended that α value larger than 1.11 be used to determine the side plate size.

5. Finite element analysis showed that the side plates could transfer approximately one third of the beam moments to the column and reduce the RI demands on the beam flange and groove-welded joint of the beam flange excluding both edges. The high RI value at the beam flange weld edges indicated minor cracks observed in the specimen tests. However, the cracks did not propagate during tests and did not adversely affect the connection seismic performance. It was further verified that only a small part of side plates near the beam flanges can effectively transfer beam flange force. A work [21] utilizing a small part of side plates near the beam flange inner side to retrofit moment connections also confirmed the effectiveness of the rehabilitation scheme.

The rehabilitation project using two steel side plates inside the beam flanges and the column face was successfully applied to the existing moment connections in the 34-story steel building in Taiwan and was completed in 2008.

ACKNOWLEDGEMENTS

The authors would like to thank the reviewers for providing valuable comments to this research.

REFERENCES

1. Engelhardt MD, Sabol TA. Testing of welded steel moment connections in response to the Northridge earthquake. *Northridge Steel Update 1*, American Institute of Steel Construction, 1994.
2. Uang CM, Bondad D. Dynamic testing of pre-Northridge and haunch repaired steel moment connections. *Report No. SSRP-96/03*, University of California, San Diego, CA, 1996.
3. Kim T, Stojadinovic B, Whittaker AS. Seismic performance of pre-Northridge welded steel moment connections to built-up box columns. *Journal of Structural Engineering* (ASCE) 2008; **134**(2):289–299.
4. Engelhardt MD, Winneberger T, Zekany AJ, Potyraj T. The dogbone connection: part II. *Modern Steel Construction*. American Institute of Steel Construction: Chicago, IL, 1996.
5. Chen SJ, Yeh CH, Chu JM. Ductile steel beam-to-column connections for seismic resistance. *Journal of Structural Engineering* (ASCE) 1996; **122**(11):1292–1299.
6. Chou CC, Wu CC. Performance evaluation of steel reduced flange plate moment connections. *Earthquake Engineering and Structural Dynamics* 2007; **36**:2083–2097.
7. Engelhardt MD, Sabol TA. Reinforcing of steel moment connections with cover plates: benefits and limitations. *Engineering Structures* 1998; **20**:510–520.
8. Uang CM, Yu QS, Noel S, Gross J. Cyclic testing of steel moment connections rehabilitated with RBS or welded haunch. *Journal of Structural Engineering* (ASCE) 2000; **126**(1):57–68.
9. Yu QS, Uang CM, Gross J. Seismic rehabilitation of steel moment connections with welded haunch. *Journal of Structural Engineering* (ASCE) 2000; **126**(1):69–78.
10. Kim T, Whittaker AS, Gilani ASJ, Bertero VV, Takhirov SM. Experimental evaluation of plate-reinforced steel moment-resisting connections. *Journal of Structural Engineering* (ASCE) 2002; **128**(4):483–491.
11. Chen CC, Chen SW, Chung MD, Lin MC. Cyclic behavior of unreinforced and rib-reinforced moment connections. *Journal of Constructional Steel Research* 2005; **61**:1–21.

DOI: 10.1002/eqe

12. Chi BC, Uang CM, Chen A. Seismic rehabilitation of pre-northridge steel moment connections: a case study. *Journal of Constructional Steel Research* 2006; **62**:783–792.
13. American Institute of Steel Construction (AISC). *Seismic Provisions for Structural Steel Buildings*, AISC, Chicago, IL, 2005.
14. Federal Emergency Management Agency (FEMA). Recommended seismic design criteria for new steel moment-frame buildings. *Report No. FEMA 350*, Federal Emergency Management Agency, Washington, DC, 2000.
15. Jao CK. Seismic behavior of steel retrofitted moment connections with stiffeners inside beam flange. *Thesis*, Thesis Advisor: Chou CC., National Chaio Tung University, Hsinchu, Taiwan, 2007.
16. Weng YT, Tsai KC, Chen PC, Chou CC, Chan YR, Jhuang SJ, Wang YY. Seismic performance evaluation of a 34-story steel building retrofitted with response modification elements. *Earthquake Engineering and Structural Dynamics* 2009; **38**:759–781.
17. Tsai KC, Wu S, Popov EP. Experimental performance of seismic steel beam–column moment joints. *Journal of Structural Engineering* (ASCE) 1995; **126**(6):925–931.
18. Chou CC, Wu CC, Jao CK, Weng YC. Weakened and strengthened steel moment connections. *4th International Conference on Earthquake Engineering*, Taipei, Taiwan, 2006. *Paper No*: *152*.
19. HKS. *ABAQUS User's Manual Version 6.3*. Hibbitt, Karlsson & Sorensen: Pawtucket, RI, 2003.
20. Structural Welding Code-Steel. American Welding Society, Miami, FL, 2006.
21. Chou CC, Jao CK. Seismic rehabilitation of welded steel moment connections to built-up box columns. *Sixth International Conference for Behavior of Steel Structures in Seismic Area*, Pennsylvania, U.S.A., 2009.
22. Hancock JW, Mackenzie AC. On the mechanism of ductile fracture in high-strength steel subjected to multi-axial stress states. *Journal of the Mechanics and Physics of Solids* 1976; **24**:147–169.

DOI: 10.1002/eqe